Low-energy three-body dynamics in binary quantum gases

O. I. Kartavtsev and A. V. Malykh

Joint Institute for Nuclear Research, Dubna, 141980, Russia

Abstract

The universal three-body dynamics in ultra-cold binary Fermi and Fermi-Bose mixtures is studied. Two identical fermions of the mass m and a particle of the mass m_1 with the zero-range two-body interaction in the states of the total angular momentum L=1 are considered. Using the boundary condition model for the s-wave interaction of different particles, both eigenvalue and scattering problems are treated by solving hyper-radial equations, whose terms are derived analytically. The dependencies of the three-body binding energies on the mass ratio m/m_1 for the positive two-body scattering length are calculated; it is shown that the ground and excited states arise at $m/m_1 \geq \lambda_1 \approx 8.17260$ and $m/m_1 \geq \lambda_2 \approx 12.91743$, respectively. For $m/m_1 \lesssim \lambda_1$ and $m/m_1 \lesssim \lambda_2$, the relevant bound states turn to narrow resonances, whose positions and widths are calculated. The 2+1 elastic scattering and the three-body recombination near the three-body threshold are studied and it is shown that a two-hump structure in the mass-ratio dependencies of the cross sections is connected with arising of the bound states.

PACS numbers: 36.10.-k, 03.75.Ss, 21.45.+v, 03.65.Ge, 34.50.-s

I. INTRODUCTION

In the last years, investigations of multi-component ultra-cold quantum gases have attracted much interest. Properties of binary Fermi-Bose [1, 2] and Fermi [3, 4, 5] mixtures and of impurities embedded in a quantum gas [6, 7]) are under experimental and theoretical study. Different aspects of the few-body dynamics of two-species compounds are of interest both from the general point of view and for many-body applications. For example, there are an infinite number of three-body bound states of two-component fermions (Efimov effect) if their mass ratio exceeds the critical value [8]. Recently, an infinite number of 1^+ bound states has been predicted [9] for three identical fermions with the resonant p-wave interaction. More detailed study of the energy spectrum of three two-component particles is of interest to shed light on the role of trimer molecules in the many-body dynamics and provides an insight into the few-body processes. Concerning the low-energy scattering, one of the interesting features is a two-hump structure in the isotopic dependence of the three-body recombination rate of two-component fermions [10, 11]. Note that the low-energy three-body recombination rate of two-component fermions scales as the first power of the collision energy and the sixth power of the two-body scattering length [10, 12].

The aim of the present paper is to study the three-body energy spectrum and the lowenergy (2+1)-scattering for two identical fermions of mass m and the third different particle of mass m_1 . Here one considers the unit total angular momentum L=1 and the s-wave interaction between different particles, which is most important for description of the lowenergy processes. Note that the s-wave interaction takes place only in binary mixtures, whereas only the p-wave interaction is possible in a one-component Fermi gas. The description of the three-body properties turns out to be universal and depending on a single parameter m/m_1 in the limit of the zero interaction range. For the interaction given within the framework of the boundary condition model (BCM), solution of hyper-radial equations (HREs) provides an efficient approach to treat both the eigenvalue and the scattering problem [13, 14, 15]. An important advantage of the BCM is that all the terms of HREs are derived in the analytical form; the method of derivation and the analytical expressions are similar to those obtained for three identical bosons in 3 and 2 dimensions [13, 16]. The calculations reveal that two three-body bound states arise while the mass ratio m/m_1 increases from zero to the critical λ_c , beyond which the number of bound states becomes infinite [8]. A two-hump structure is found for the mass-ratio dependencies of the elastic and inelastic (2 + 1)-scattering cross sections near the three-body threshold. The structure of the isotopic dependencies is qualitatively related to arising of the bound states as a common origin is an increase of the potential-well depth in the 2 + 1 channel.

II. OUTLINE OF THE APPROACH

In the universal low-energy limit, the short-range two-body interaction is described by a single parameter, a natural choice for which is the two-body scattering length a. For the vanishing range of interaction, the two-body interaction is defined within the framework of the BCM by imposing the boundary condition at the zero inter-particle distance r

$$\lim_{r \to 0} \frac{\partial \ln(r\Psi)}{\partial r} = -\frac{1}{a} \ . \tag{1}$$

The two-body interaction introduced in this way is known in the literature as the zero-range potential [17], the Fermi pseudo-potential [18], the Fermi-Huang pseudo-potential [19, 20], and an equivalent approach is used in the momentum-space representation [21].

For definiteness, one supposes that particle 1 is of mass m_1 and particles 2 and 3 are two identical fermions of mass m. The wave function Ψ satisfies the equation

$$[\Delta_{\mathbf{x}} + \Delta_{\mathbf{y}} + E]\Psi = 0 , \qquad (2)$$

where the scaled Jacobi variables $\mathbf{x} = \sqrt{2\mu} \left(\mathbf{r}_2 - \mathbf{r}_1 \right)$ and $\mathbf{y} = \sqrt{2\tilde{\mu}} \left(\mathbf{r}_3 - \frac{m_1 \mathbf{r}_1 + m \mathbf{r}_2}{m_1 + m} \right)$ are defined via the position vectors \mathbf{r}_i and the reduced masses $\mu = \frac{m m_1}{m + m_1}$ and $\tilde{\mu} = \frac{m(m + m_1)}{m_1 + 2m}$. The total interaction is expressed by imposing two boundary conditions of the form (1) at zero distances between the different particles in two pairs 1 - 2 and 1 - 3. One demands that the wave function should be antisymmetric under permutation of identical fermions 2 and 3; under this condition only a single boundary condition of the form (1) should be imposed at the zero distance between particles 1 and 2, $x \to 0$. The unit total angular momentum L = 1 is considered, which is most important for the low-energy processes [10, 12]. The units $\hbar = 2\mu = |a| = 1$ will be used hereafter; thus, any three-body property depends only on the single remaining parameter m/m_1 .

The three-body bound and resonance states and the low-energy scattering are conveniently treated by solving a system of HREs [22]. The eigenfunctions $\Phi_n(\rho, \Omega)$ are defined

as regular solutions on the hypersphere at the fixed hyper-radius ρ ,

$$\left[\frac{1}{\sin^2 2\alpha} \left(\sin^2 2\alpha \frac{\partial}{\partial \alpha}\right) + \frac{1}{\sin^2 \alpha} \Delta_{\hat{\mathbf{x}}} + \frac{1}{\cos^2 \alpha} \Delta_{\hat{\mathbf{y}}} + \gamma_n^2(\rho) - 4\right] \Phi_n(\rho, \Omega) = 0 , \qquad (3)$$

$$\lim_{\alpha \to 0} \left[\frac{\partial \ln \left(\alpha \Phi_n \right)}{\partial \alpha} \pm \rho \right] = 0 , \qquad (4)$$

where Ω is a brief notation for the hyper-angles α , $\hat{\mathbf{x}}$, and $\hat{\mathbf{y}}$. The hyper-spherical variables are defined by the relations $x = \rho \sin \alpha$, $y = \rho \cos \alpha$, $\hat{\mathbf{x}} = \mathbf{x}/x$, and $\hat{\mathbf{y}} = \mathbf{y}/y$. The \pm sign in (4), which corresponds to the positive and negative scattering length a, hereafter will be incorporated into the parameter ρ . Thus, the eigenvalue problem will be considered for an arbitrary $-\infty < \rho < \infty$. For each value of ρ , the solution of (3) and (4) determines a set of discrete eigenvalues $\gamma_n^2(\rho)$, which are enumerated in ascending order by an index $n = 1, 2, 3, \ldots$, and corresponding eigenfunctions $\Phi_n(\rho, \Omega)$. The expansion of the total wave function in a set of eigenfunctions $\Phi_n(\rho, \Omega)$ normalized by the condition $\langle \Phi_n | \Phi_m \rangle = \delta_{nm}$,

$$\Psi = \rho^{-5/2} \sum_{n=1}^{\infty} f_n(\rho) \Phi_n(\rho, \Omega) , \qquad (5)$$

leads to an infinite set of coupled HREs

$$\left[\frac{d^2}{d\rho^2} - \frac{\gamma_n^2(\rho) - 1/4}{\rho^2} + E\right] f_n(\rho) - \sum_{m=1}^{\infty} \left[P_{mn}(\rho) - Q_{mn}(\rho) \frac{d}{d\rho} - \frac{d}{d\rho} Q_{mn}(\rho) \right] f_m(\rho) = 0 , \quad (6)$$

where

$$Q_{nm}(\rho) = \left\langle \Phi_n \middle| \frac{\partial \Phi_m}{\partial \rho} \right\rangle , \quad P_{nm}(\rho) = \left\langle \frac{\partial \Phi_n}{\partial \rho} \middle| \frac{\partial \Phi_m}{\partial \rho} \right\rangle , \tag{7}$$

and the notation $\langle \cdot | \cdot \rangle$ stands for integration over the invariant volume on the hypersphere $d\Omega = \sin^2 2\alpha \, d\alpha \, d\hat{\mathbf{x}} d\hat{\mathbf{y}}$.

The eigenfunctions $\Phi_n(\rho, \Omega)$ inherit the antisymmetry of the wave function under permutation of the identical fermions 2 and 3. The solutions of the eigenvalue problem (3) and (4), which satisfy the permutational symmetry and belong to the total angular momentum L=1 and its projection M, are expressed as

$$\Phi_n(\rho, \Omega) = \left(1 - \widehat{P}\right) \frac{\varphi_n(\alpha, \rho)}{\sin 2\alpha} Y_{1M}(\hat{\mathbf{y}}) , \qquad (8)$$

where $Y_{LM}(\hat{\mathbf{y}})$ is the spherical function and \widehat{P} denotes the permutation of particles 2 and 3. The action of \widehat{P} in terms of the Jacobi variables is given by

$$\widehat{P}\mathbf{x} = -\sin\omega\mathbf{x} + \cos\omega\mathbf{y} , \quad \widehat{P}\mathbf{y} = -\cos\omega\mathbf{x} - \sin\omega\mathbf{y} , \qquad (9)$$

where the angle of the kinematic rotation ω is expressed via the mass ratio as $\cot \omega = (m_1/m)\sqrt{1+2m/m_1}$. Given the representation (8), the eigenvalue problem (3) and (4) is reduced to the equation

$$\left[\frac{\partial^2}{\partial \alpha^2} - \frac{2}{\cos^2 \alpha} + \gamma_n^2(\rho)\right] \varphi_n(\alpha, \rho) = 0$$
 (10)

complemented by the boundary conditions $\varphi(\alpha, \rho) = 0$ at $\alpha = \pi/2$ and

$$\lim_{\alpha \to 0} \left(\frac{\partial}{\partial \alpha} + \rho \right) \varphi_n(\alpha, \rho) + \frac{2}{\sin 2\omega} \varphi_n(\omega, \rho) = 0 , \qquad (11)$$

at the singular point $\alpha = 0$ of the eigenfunctions $\Phi_n(\rho, \Omega)$. The boundary condition (11) is deduced from Eqs. (4), (8), and (9) by observing that $\widehat{P}\alpha \to \pi/2 - \omega$ and $\widehat{P}Y_{1M}(\hat{\mathbf{y}}) \to -Y_{1M}(\hat{\mathbf{y}})$ as $\alpha \to 0$.

The zero-valued at $\alpha=\pi/2$ unnormalized solutions to Eq. (10) are straightforwardly written as

$$\varphi_n(\alpha, \rho) = \gamma_n(\rho) \cos \left[\gamma_n(\rho) \left(\pi/2 - \alpha\right)\right] - \tan \alpha \sin \left[\gamma_n(\rho) \left(\pi/2 - \alpha\right)\right] . \tag{12}$$

Substituting (12) into the boundary condition (11), one eventually finds the transcendental equation,

$$\rho = \frac{1 - \gamma^2}{\gamma} \tan \gamma \frac{\pi}{2} - \frac{2}{\sin 2\omega} \frac{\cos \gamma \omega}{\cos \gamma \frac{\pi}{2}} + \frac{\sin \gamma \omega}{\gamma \sin^2 \omega \cos \gamma \frac{\pi}{2}} , \qquad (13)$$

which determines the infinitely multivalued function $\gamma^2(\rho)$ of an arbitrary complex-valued variable ρ at various mass ratios m/m_1 given by the parameter ω . Different branches of this unique function for the real-valued ρ form a set of real-valued eigenvalues $\gamma_n^2(\rho)$; thus, the solution of the eigenvalue problem is accomplished by means of expressions (12) and (13).

An advantage of the BCM is that the eigenvalues $\gamma_n^2(\rho)$ entering into HREs are expressed in a simple analytical form [14, 15, 16], which is helpful both for qualitative analysis and in the numerical calculations. Moreover, the coupling terms $Q_{nm}(\rho)$ and $P_{nm}(\rho)$ can be determined in the analytical form via $\gamma_n^2(\rho)$ and their derivatives as was done in [13, 16]; the derivation is outlined in the Appendix.

Properties of the eigenvalues $\gamma_n^2(\rho)$ are deduced by analyzing Eq. (13), in particular, all the $\gamma_n^2(\rho)$ monotonically decrease within the intervals $9 > \gamma_1^2(\rho) > -\infty$ and $(2n+1)^2 > \gamma_n^2(\rho) > (2n-1)^2$ for $n \geq 2$ as the hyper-radius runs the interval $-\infty < \rho < \infty$. The effective potentials in the upper channels for $n \geq 2$ contain the repulsive term $\gamma_n^2(\rho)/\rho^2$, which

means a dominant role of the lowest channel for the low-energy solutions. Furthermore, the first-channel potential at small ρ is approximately determined by $\gamma_1^2(0)$ so that $V_1(\rho) \approx [\gamma_1^2(0) - 1/4]/\rho^2$, which entails that a number of the bound states is finite for $\gamma_1^2(0) > 0$ and infinite for $\gamma_1^2(0) < 0$. As follows from Eq. (13), $\gamma_1^2(0)$ decreases with increasing ω and crosses zero at the critical value $\omega_c \approx 1.19862376$, which satisfies the equation

$$\frac{\pi}{2}\sin^2\omega_c - \tan\omega_c + \omega_c = 0 , \qquad (14)$$

and corresponds to the critical mass ratio $\lambda_c \approx 13.6069657$. Thus, one concludes that a number of three-body bound states is either finite or infinite if the mass ratio m/m_1 is below or above λ_c . An infinite energy spectrum of three fermions for the mass ratio above the critical value, $m/m_1 > \lambda_c$, was first discovered in Ref. [8]. Note that the unambiguous description of the three-body properties for $m/m_1 > \lambda_c$ requires an additional parameter which determines the wave function in the vicinity of the triple-collision point.

More detailed analysis is needed to describe the energy spectrum for the mass ratio below the critical value, $m/m_1 \leq \lambda_c$. The description is quite simple for the negative two-body scattering length a < 0, in which case all the $\gamma_n^2(\rho)$ are non-negative for $m/m_1 \leq \lambda_c$, which means unboundedness of the three particles. Considering the positive two-body scattering length a > 0, one finds that there are no bound states for the small enough mass ratio roughly below 5 because the first-channel diagonal term $\gamma_1^2(\rho)/\rho^2$ exceeds the threshold energy E = -1 for those $m/m_1 \lesssim 5$. To estimate the number of the bound states which occur as m/m_1 increases to the critical mass ratio λ_c , one should consider the small- ρ behaviour of the eigenvalue $\gamma_1^2(\rho) \approx -q_c \rho$ at $m/m_1 = \lambda_c$. Correspondingly, the first-channel diagonal term is of the form $-\frac{1}{4\rho^2} - \frac{q_c}{\rho}$, where $q_c = \left[\frac{\pi}{2}\left(1 + \frac{\pi^2}{24} - \frac{\omega_c^2}{2}\right) - \frac{\omega_c^3}{3\sin^2\omega_c}\right]^{-1} \approx 2.34253823$. As the energy of the nth level in this potential is $E_n = -q_c^2/(2n-1)^2$, one can roughly estimate that at least one and not more than two bound states exist for $m/m_1 = \lambda_c$. To illustrate the above-described properties, two lowest terms $\gamma_n^2(\rho)/\rho^2$ of HREs are depicted in Fig. 1 for different values of the mass ratio.

The asymptotic expressions for the channel potentials $V_n(\rho) = \frac{\gamma_n^2(\rho) - 1/4}{\rho^2} + P_{nn}(\rho)$ and the coupling terms $P_{nm}(\rho)$ and $Q_{nm}(\rho)$ are of interest for solution of both the eigenvalue and the scattering problem. The asymptotic form of $\gamma_n^2(\rho)$ at a large hyper-radius is determined

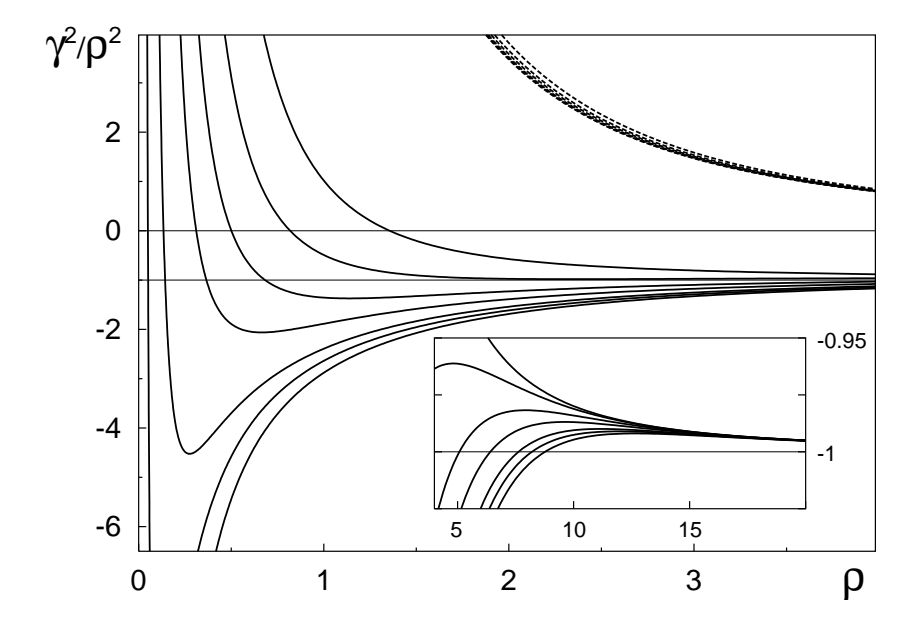


FIG. 1: Diagonal terms in HREs $\gamma_1^2(\rho)/\rho^2$ (solid lines) and $\gamma_2^2(\rho)/\rho^2$ (dashed lines) for a set of mass ratios $m/m_1 = 1, 5, 8, 10, 12, 13, 14$ (top to bottom). In the inset the first-channel terms are shown on a large scale in the barrier region. For reference, the two-body threshold at E = -1 is plotted.

by the expansion of Eq. (13) for $\gamma \to i\infty$ and $\gamma \to 2n-1$, which gives

$$\gamma_n^2(\rho) = \begin{cases} -\rho^2 + 2 + O(\rho^{-2}) &, n = 1, \\ (2n-1)^2 + c_n/\rho + O(\rho^{-2}) &, n > 1, \end{cases}$$
 (15)

where $c_n = \frac{4}{\pi} \left[\frac{4n(n-1)}{2n-1} - 2\frac{(-1)^n \cos(2n-1)\omega}{\sin 2\omega} + \frac{(-1)^n \sin(2n-1)\omega}{(2n-1)\sin^2 \omega} \right]$. Substituting Eq. (15) in the exact expressions (A7), (A9), and (A13) one obtains a large- ρ expansion for the coupling terms, $P_{11}(\rho) = 1/(4\rho^2) + O(\rho^{-6})$, $Q_{n1}(\rho) = O(\rho^{-5/2})$, $P_{n1}(\rho) = O(\rho^{-5/2})$, $Q_{nm}(\rho) = O(\rho^{-2})$, and $P_{nm}(\rho) = O(\rho^{-4})$ for $n, m \neq 1$. The channel potentials take the asymptotic form

$$V_1(\rho) = -1 + \frac{2}{\rho^2} + O(\rho^{-4}) \tag{16}$$

and

$$V_n(\rho) = \frac{(2n - 1/2)(2n - 3/2)}{\rho^2} + O(\rho^{-4}), \quad n \ge 2 ,$$
 (17)

which corresponds to the long-range interaction of a dimer with the third particle for n = 1 and of three asymptotically free particles for $n \ge 2$.

In addition to the above-described qualitative conclusions, a detailed quantitative description of the three-body properties will be given for the non-trivial case a > 0 and $m/m_1 \le \lambda_c$. In the following sections both the energy spectrum and the scattering characteristics are obtained by the numerical solution of HREs (6) complemented by the natural zero boundary conditions $f_n(\rho) \to 0$ as $\rho \to 0$ and the specified asymptotic boundary conditions as $\rho \to \infty$. All the terms of HREs are calculated by using the eigenvalue equation (13) and the exact expressions (A7), (A9), and (A13) for the coupling terms, which provides a high accuracy of the numerical results.

III. THREE-BODY BOUND STATES AND NEAR-THRESHOLD RESONANCES

The dependencies of the three-body binding energies on the mass ratio are determined by solving a system of HREs with the zero asymptotic boundary conditions, $f_n(\rho) \to 0$ as $\rho \to \infty$. The results of the calculations are shown in Fig. 2 and in Table I; it turns out that there are zero, one, and two bound states for $0 < m/m_1 < \lambda_1$, $\lambda_1 \le m/m_1 < \lambda_2$ and $\lambda_2 \le m/m_1 \le \lambda_c$, respectively. The binding energies increase as the mass ratio

TABLE I: Mass ratios λ_i for which the three-body bound states arise and energies E_{ic} of these states for $m/m_1 = \lambda_c$ calculated with N HREs.

```
N
      \lambda_1
                 \lambda_2
                           E_{1c}
                                     E_{2c}
1 8.183854 12.929430 -5.89405 -1.13632
2 8.175776 12.921084 -5.89525 -1.13730
3 8.173692 12.918879 -5.89537 -1.13752
4 8.173003 12.918061 -5.89540 -1.13759
5 8.172771 12.917712 -5.89541 -1.13762
6 8.172688 12.917564 -5.89542 -1.13763
7 8.172651 12.917500
8 8.172633 12.917473
9\ \ 8.172622\ 12.917457\ \text{-}5.89542\ \text{-}1.13764
12\ 8.172608\ 12.917436
\infty 8.17260 12.91743
```

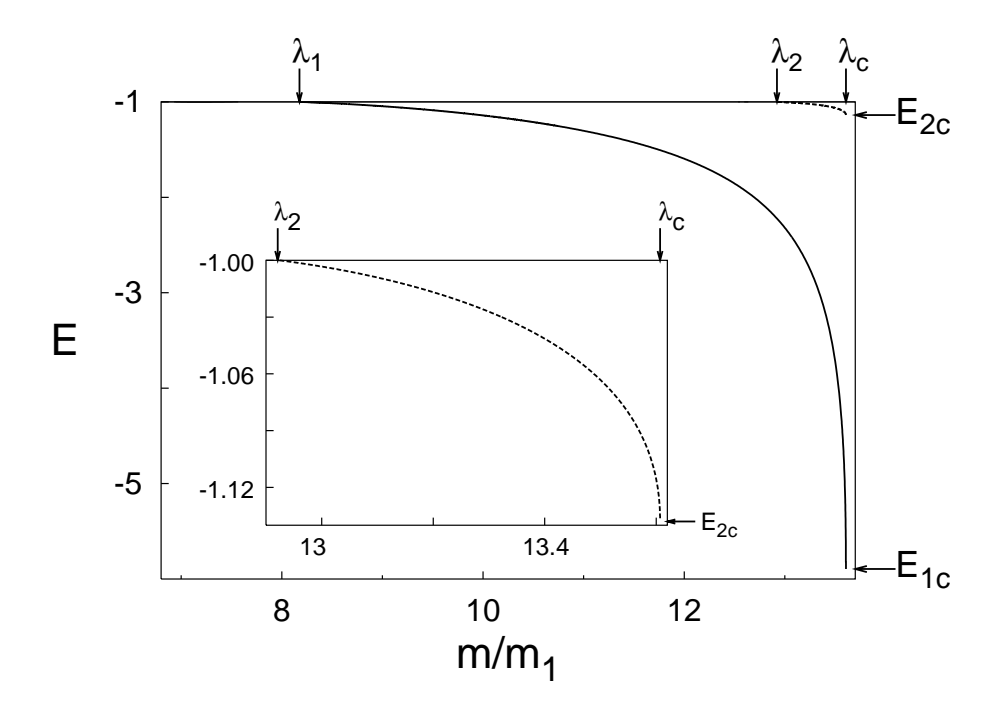


FIG. 2: Dependencies of the bound-state energies (in units of the two-body binding energy) on the mass ratio m/m_1 . The arrows mark the mass ratios λ_i , for which the *i*th bound state emerges from the two-body threshold, the critical mass ratio λ_c , and the bound-state energies E_{ic} for $m/m_1 = \lambda_c$. In the inset the excited-state energy is shown on a large scale.

increases to the critical value λ_c ; in the limit $m/m_1 \to \lambda_c$ the energies tend to the finite values E_{ic} (i=1,2) following a square-root dependence $E_i - E_{ic} \propto \sqrt{\lambda_c - m/m_1}$, which is demonstrated in Fig. 3. Notice that this mass-ratio dependence comes from the expansion $\gamma_1^2(0) \propto \lambda_c - m/m_1$ as $m/m_1 \to \lambda_c$.

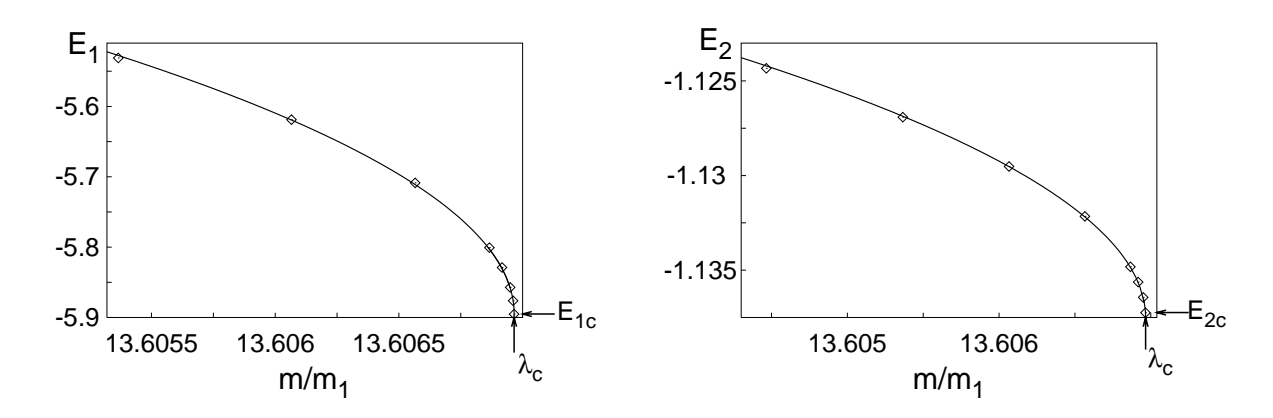


FIG. 3: Calculated ground-state and excited-state energies (diamonds) for $m/m_1 \lesssim \lambda_c$ fitted to the square-root dependence $E - E_c \propto \sqrt{\lambda_c - m/m_1}$ (lines).

For the mass ratios λ_i , at which the three-body bound states arise, there are true bound states at the threshold energy E=-1, whose wave functions are square-integrable with a power fall-off at large distances. Thus, to calculate the precise values λ_i , a system of HREs is solved for E=-1 by using the power dependence of the first-channel function, $f_1(\rho) \sim \rho^{-2}$ as $\rho \to \infty$. The calculated λ_i rapidly converge with increasing number of HREs N, being fairly well fitted to the power dependence $a+b/N^c$ with $c\approx 4$; the dependencies of λ_i on N and the fitted values in the limit $N\to\infty$ are presented in Table I. If the mass ratio slightly exceeds λ_i , the separation of the loosely bound state from the two-body threshold is proportional to the mass ratio excess, viz., $|E_i+1|\propto m/m_1-\lambda_i$. For the mass ratio just below λ_i , the relevant bound state turns to a narrow resonance, whose position E_i^r continues a linear mass-ratio dependence of the bound-state energy, $E_i^r+1\propto \lambda_i-m/m_1$, whereas the width Γ_i depends quadratically on the mass ratio excess, $\Gamma_i\propto (\lambda_i-m/m_1)^2$. The above-described threshold features are connected with the presence of the long-range term $2/\rho^2$ in the (2+1)-channel effective potential (illustrated in the inset of Fig. 1).

To calculate the positions and widths of two narrow resonances for $m/m_1 \lesssim \lambda_i$, a system of HREs is solved for $E \gtrsim -1$. In view of Eq. (16), the asymptotic boundary condition for $\rho \to \infty$ imposed to allow for the incoming and outgoing waves in the first channel is taken in the form

$$f_1(\rho) \to \rho \left[j_1(k\rho) - \tan \delta(k) y_1(k\rho) \right] ,$$
 (18)

where the wave number k is given by $E = -1 + k^2$, $\delta(k)$ is the (2 + 1)-scattering phase shift, and $j_1(x)$ and $y_1(x)$ are the spherical Bessel functions. The resonance position E_r and the width Γ are determined by fitting $\delta(k)$ to the Wigner dependence,

$$\cot[\delta(k) - \delta_{bg}] = \frac{2}{\Gamma}(E^r - E) , \qquad (19)$$

where δ_{bg} is the non-resonant phase shift. Near-threshold mass-ratio dependencies of the bound-state energies E_i and the resonance parameters E_i^r and Γ_i are shown in Fig. 4.

IV. LOW-ENERGY SCATTERING NEAR THE THREE-BODY THRESHOLD

The scattering problem at small energies near the three-body threshold is solved in the two-channel approximation for the mass ratio within the range $0 \le m/m_1 \le \lambda_c$. The K-matrix is calculated by using two independent solutions $f^{(1)}$ and $f^{(2)}$, which satisfy, in view

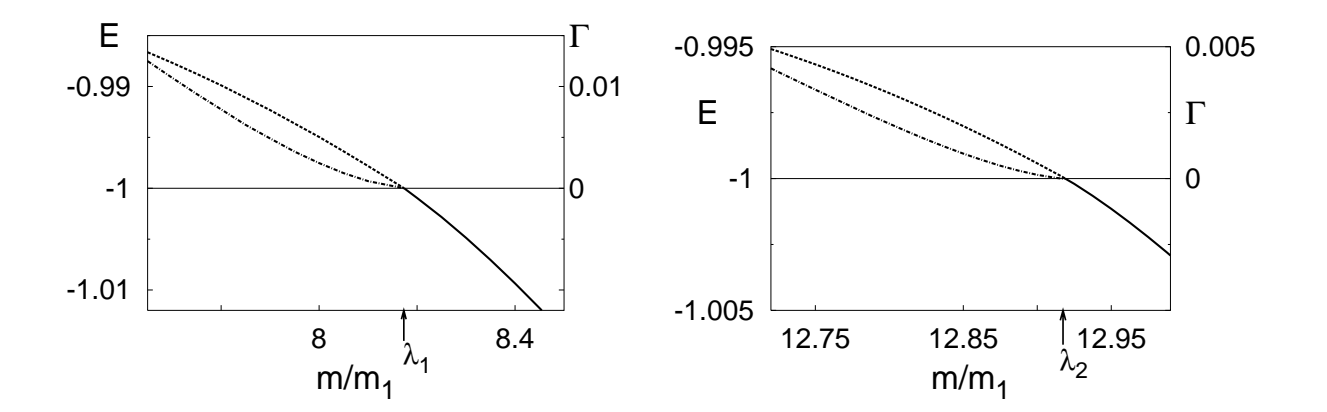


FIG. 4: Near-threshold mass-ratio dependencies of the bound-state energies E_i (bold solid lines), resonance positions E_i^r (thin solid lines), and resonance widths Γ_i (dashed lines).

of Eq. (16) and (17), the following asymptotic boundary conditions

$$[f^{(1)}, f^{(2)}] = \sqrt{\rho} \begin{bmatrix} Y_{3/2}(k\rho) & 0 \\ 0 & Y_3(\sqrt{k^2 - 1}\rho) \end{bmatrix} + K \begin{pmatrix} J_{3/2}(k\rho) & 0 \\ 0 & J_3(\sqrt{k^2 - 1}\rho) \end{pmatrix}$$
(20)

as $\rho \to \infty$. The elastic (2+1)-scattering phase shift is defined by $\cot \delta(k) = -K_{11}(k)$ and the inelastic scattering amplitude is determined by the non-diagonal element of the T-matrix given by $T = 2(1 - iK)^{-1}$. The elastic-scattering phase shift at the three-body threshold $\delta_{th} \equiv \delta(1)$ is a smooth increasing function of m/m_1 , which takes the value between $3\pi/2$ and 2π at $m/m_1 = \lambda_c$. Correspondingly, the elastic-scattering cross section at the three-body threshold is determined in the dimensional units as $\sigma_{th} = 12\pi a^2 \frac{(1+2m/m_1)}{(1+m/m_1)^2} \sin^2 \delta_{th}$. As shown in Fig. 5, the mass-ratio dependence of σ_{th} is a two-hump structure with two maximums located near those values m/m_1 at which δ_{th} passes through $\pi/2$ and $3\pi/2$.

The low-energy dependence of the three-body recombination rate α_r is determined by the squared non-diagonal T-matrix element as $\alpha_r \sim |T_{21}(E)|^2 E^{-2}$. For small $E \to 0$, the numerical calculations corroborate the dependence $T_{21}(E) = E^{3/2}(A + BE)$, which agrees with the linear low-energy behaviour $\alpha_r \sim A^2 E$ described in Refs. [10, 12]. The mass-ratio dependence of the leading-order term A^2 , which determines the three-body recombination rate at low energy, is shown in Fig. 5. A two-hump structure of $A^2(m/m_1)$ with two maxima and three zeros within the interval $0 \le m/m_1 \le \lambda_c$ is in agreement with the result of Ref. [10].

A similar structure of both dependencies $\sigma_{th}(m/m_1)$ and $A^2(m/m_1)$ originates from the interference of the incoming and outgoing waves in the 2+1 channel, being closely connected

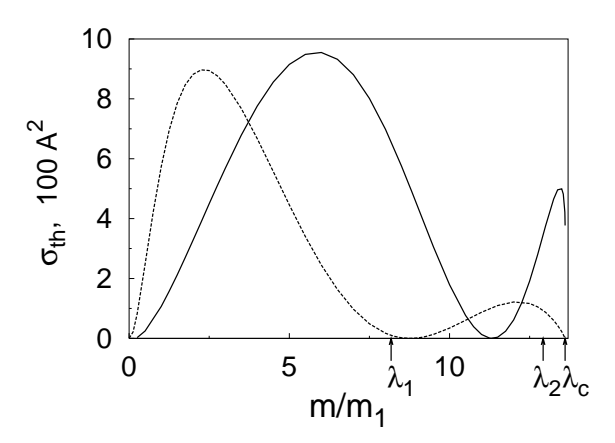


FIG. 5: Mass-ratio dependencies of the elastic (2+1)-scattering cross section at the three-body threshold σ_{th} (solid line) and the low-energy leading-order term $A^2 = \lim_{E \to 0} |T_{21}|^2 E^{-3}$ of the three-body recombination rate $\alpha_r \sim A^2 E$ (dashed line).

with the potential-well deepening as m/m_1 increases. Qualitatively, the (2 + 1)-channel function $f_1(\rho)$ acquires additional oscillations as the potential-well depth increases, which leads to an oscillating mass-ratio dependence of both elastic and inelastic scattering amplitudes. On the other hand, arising of the three-body bound states with increasing m/m_1 is connected with occurrence of oscillations of $f_1(\rho)$ within the potential-well range. In this respect, one can mention an analogy with Levinson's theorem, which links the number of the bound states to the threshold-energy phase shift.

V. DISCUSSION

The universal low-energy description for two identical fermions interacting with the third different particle in the states of the total angular momentum L=1 is given within the framework of the approach based on the solution of hyper-radial equations, whose terms are derived in the analytical form. It is found that there are no three-body bound-states for the negative scattering length and $m/m_1 \leq \lambda_c$, whereas for the positive scattering length there are exactly zero, one and two bound states for $m/m_1 < \lambda_1$, $\lambda_1 \leq m/m_1 < \lambda_2$ and $\lambda_2 \leq m/m_1 \leq \lambda_c$, respectively. For m/m_1 just below λ_1 or λ_2 , the bound states disappear and turn to narrow resonances, whose positions and widths are calculated.

The above-described universal picture should be observed in the limit $|a| \to \infty$, i. e., if the potential is tuned to produce the loosely bound two-body state. In this limit, one

expects to observe simultaneously the loosely bound two-body and three-body states, whose binding energies scale as a^{-2} and their ratio depends on m/m_1 . Similar threshold behaviour of the binding energies was discussed in [16, 23, 24] for three two-dimensional bosons.

Both the elastic (2 + 1)-scattering cross sections and the three-body recombination rate near the three-body threshold manifest a two-hump structure of their mass-ratio dependencies for $m/m_1 \leq \lambda_c$. The structure of both isotopic dependencies stems from the interference of the incoming and outgoing waves due to deepening of the effective potential in the 2 + 1channel; in this respect, the interference is connected with arising of two three-body bound states with increasing m/m_1 .

As the present paper describes the universal three-body properties in the idealized limit of the zero interaction range, it is of interest to discuss briefly the effect of the finite, though small enough interaction radius $r_0 \ll a$. For the mass ratio below the critical value λ_c , the binding energies depend smoothly on the interaction radius r_0 and on the interaction in the vicinity of the triple-collision point provided $r_0 \ll a$, whereas for $m/m_1 > \lambda_c$ the infinite energy spectrum is extremely sensitive to these parameters. Furthermore, an abrupt transition from two to an infinite number of bound states at $m/m_1 = \lambda_c$ will be smeared off if either the interaction range is not zero or the three-body force is present. One can roughly estimate that the number of three-body bound states $N_b = 2$ for the mass ratio within the range $m/m_1 - \lambda_c \lesssim r_0/a$ and increases as $N_b \propto \sqrt{m/m_1 - \lambda_c} \ln \frac{a}{r_0}$ with increasing m/m_1 .

Finally, it is worth noting that the p-wave trimer molecule containing two heavy fermions and the light third particle could be observed in the ultra-cold mixtures of 87 Sr with lithium isotopes. For the mixtures of 87 Sr with 7 Li, the mass ratio $m/m_1 \approx 12.4 > \lambda_1$, which entails existence of the trimer bosonic molecule 7 Li 87 Sr₂, whose binding energy is about 0.793 times the binding energy of the dimer molecule 7 Li 87 Sr. For the mixtures of 87 Sr with 6 Li, the mass ratio $m/m_1 = 14.5$ slightly exceeds the critical value λ_c , which entails existence of the trimer fermionic molecule 6 Li 87 Sr₂ in two states, whose binding energies are slightly above 4.895 and 0.138 times the binding energy of the dimer molecule 6 Li 87 Sr.

Acknowledgement. Support by the grant of "Econatsbank" and the Votruba-Blokhintsev grant is gratefully acknowledged.

APPENDIX A: ANALYTICAL EXPRESSIONS FOR THE COUPLING TERMS

Although the direct calculation of the coupling terms $Q_{nm}(R)$ and $P_{nm}(R)$ via the definition (7) is quite involved, one can circumvent this problem and obtain the analytical expressions for $Q_{nm}(\rho)$ and $P_{nm}(\rho)$ via $\gamma_n^2(\rho)$ and their derivatives by using the explicit dependence on ρ in the boundary condition (4). Similar analytical expressions were derived for a number of problems based on the BCM; more details are given in [16].

Hereafter one concisely writes the eigenvalue problem (3), (4) as

$$\left(\tilde{\Delta} + \gamma_n^2\right) \Phi_n = 0 , \qquad (A1)$$

$$\lim_{\alpha \to 0} \left(\frac{\partial}{\partial \alpha} + \rho \right) \sin 2\alpha \Phi_n = 0 . \tag{A2}$$

The derivative of the normalized eigenfunction Φ_n with respect to ρ satisfies the inhomogeneous equation

$$\left(\tilde{\Delta} + \gamma_n^2\right) \frac{\partial \Phi_n}{\partial \rho} + \frac{d\gamma_n^2}{d\rho} \Phi_n = 0 \tag{A3}$$

and the boundary condition

$$\lim_{\alpha \to 0} \left[\left(\frac{\partial}{\partial \alpha} + \rho \right) \sin 2\alpha \frac{\partial \Phi_n}{\partial \rho} + \sin 2\alpha \Phi_n \right] = 0 . \tag{A4}$$

By projecting Eq. (A3) onto Φ_m and using the representation (8) one obtains the relation,

$$(\gamma_n^2 - \gamma_m^2)Q_{mn} + \delta_{nm}\frac{d\gamma_n^2}{d\rho} + \varphi_n(0,\rho)\varphi_m(0,\rho) = 0 , \qquad (A5)$$

where the integrals over the hypersphere are expressed via the integrals over the hypersurfaces surrounding two singularities of the functions Φ_n , viz., one at $\alpha = 0$ and the other given by the permutational symmetry. Here the integration volume is arbitrarily chosen to provide the unit coefficient for the last term in (A5) and it is taken into account that equal contributions come from two surface integrals around both singularities. The diagonal part of Eq. (A5) gives the basic relation

$$\varphi_n^2(0,\rho) = -\frac{d\gamma_n^2}{d\rho} \,, \tag{A6}$$

which allows one to derive the desired expressions via the derivative of the eigenvalues $\gamma_n^2(\rho)$. Substituting (A6) in the non-diagonal part of (A5), one finds

$$Q_{nm} = \left(\gamma_n^2 - \gamma_m^2\right)^{-1} \sqrt{\frac{d\gamma_n^2}{d\rho} \frac{d\gamma_m^2}{d\rho}} \ . \tag{A7}$$

In a similar way, the projection of Eq. (A3) onto $\frac{\partial \Phi_m}{\partial \rho}$ for $n \neq m$ leads to the relation

$$\frac{d(\gamma_n^2 + \gamma_m^2)}{d\rho} Q_{mn} = (\gamma_n^2 - \gamma_m^2) P_{mn} + \varphi_n(0, \rho) \frac{d\varphi_m(0, \rho)}{d\rho} - \varphi_m(0, \rho) \frac{d\varphi_n(0, \rho)}{d\rho} , \qquad (A8)$$

which is finally transformed to the expression for the non-diagonal coupling terms

$$P_{nm} = Q_{nm} \left[\left(\gamma_m^2 - \gamma_n^2 \right)^{-1} \frac{d}{d\rho} \left(\gamma_n^2 + \gamma_m^2 \right) + \frac{1}{2} \frac{d^2 \gamma_n^2}{d\rho^2} \left(\frac{d\gamma_n^2}{d\rho} \right)^{-1} - \frac{1}{2} \frac{d^2 \gamma_m^2}{d\rho^2} \left(\frac{d\gamma_m^2}{d\rho} \right)^{-1} \right] , \quad (A9)$$

where one uses Eq. (A6) and its derivative $\frac{d^2\gamma_n^2}{d\rho^2} = -2\varphi_n(0,\rho)\frac{d\varphi_n(0,\rho)}{d\rho}$.

At last, the second derivative of the eigenfunction Φ_n with respect to ρ satisfies the equation

$$\left(\tilde{\Delta} + \gamma_n^2\right) \frac{\partial^2 \Phi_n}{\partial \rho^2} + 2 \frac{d\gamma_n^2}{d\rho} \frac{\partial \Phi_n}{\partial \rho} + \frac{d^2 \gamma_n^2}{d\rho^2} \Phi_n = 0 \tag{A10}$$

and the boundary condition

$$\lim_{\alpha \to 0} \left[\left(\frac{\partial}{\partial \alpha} + \rho \right) \sin 2\alpha \frac{\partial^2 \Phi_n}{\partial \rho^2} + 2 \sin 2\alpha \frac{\partial \Phi_n}{\partial \rho} \right] = 0 . \tag{A11}$$

By projecting Eq. (A10) onto Φ_n and using the identity $P_{nn} = -\left\langle \Phi_n \middle| \frac{\partial^2 \Phi_n}{\partial \rho^2} \right\rangle$, one finds that

$$3\frac{d\gamma_n^2}{d\rho}P_{nn} = \varphi_n(0,\rho)\frac{d^2\varphi_n(0,\rho)}{d\rho^2} - 2\left[\frac{d\varphi_n(0,\rho)}{d\rho}\right]^2. \tag{A12}$$

The derivatives of $\varphi_n(0,\rho)$ are expressed via the derivatives of $\gamma_n^2(\rho)$ by using Eq. (A6), which allows one to cast the diagonal coupling term in the form

$$P_{nn} = -\frac{1}{6} \frac{d^3 \gamma_n^2}{d\rho^3} \left(\frac{d\gamma_n^2}{d\rho}\right)^{-1} + \frac{1}{4} \left(\frac{d^2 \gamma_n^2}{d\rho^2}\right)^2 \left(\frac{d\gamma_n^2}{d\rho}\right)^{-2} . \tag{A13}$$

- [1] C. Ospelkaus, S. Ospelkaus, K. Sengstock, and K. Bongs, Phys. Rev. Lett. 96, 020401 (2006).
- [2] T. Karpiuk, M. Brewczyk, M. Gajda, and K. Rzazewski, Journ. Phys. B 38, L215 (2005).
- [3] Y. Shin, M. W. Zwierlein, C. H. Schunck, A. Schirotzek, and W. Ketterle, Phys. Rev. Lett. 97, 030401 (2006).
- [4] F. Chevy, Phys. Rev. Lett. **96**, 130401 (2006).
- [5] M. Iskin and C. A. R. S. de Melo, Phys. Rev. Lett. 97, 100404 (2006).
- [6] F. M. Cucchietti and E. Timmermans, Phys. Rev. Lett. **96**, 210401 (2006).

- [7] R. M. Kalas and D. Blume, Phys. Rev. A 73, 043608 (2006).
- [8] V. Efimov, Nucl. Phys. A **210**, 157 (1973).
- [9] J. H. Macek and J. Sternberg, Phys. Rev. Lett. **97**, 023201 (2006).
- [10] D. S. Petrov, Phys. Rev. A **67**, 010703(R) (2003).
- [11] D. S. Petrov, C. Salomon, and G. V. Shlyapnikov, Phys. Rev. A 71, 012708 (2005).
- [12] H. Suno, B. D. Esry, and C. H. Greene, Phys. Rev. Lett. **90**, 053202 (2003).
- [13] O. I. Kartavtsev, Few-Body Syst. Suppl. **10**, 199 (1999).
- [14] E. Nielsen, D. V. Fedorov, and A. S. Jensen, Few-Body Syst. 27, 15 (1999).
- [15] O. I. Kartavtsev and J. H. Macek, Few-Body Syst. 31, 249 (2002).
- [16] O. I. Kartavtsev and A. V. Malykh, Phys. Rev. A 74, 042506 (2006).
- [17] Y. N. Demkov and V. N. Ostrovskii, Zero-range potentials and their applications in atomic physics (Plenum Press, New York, 1988).
- [18] K. Wódkiewicz, Phys. Rev. A 43, 68 (1991).
- [19] Z. Idziaszek and T. Calarco, Phys. Rev. Lett. **96**, 013201 (2006).
- [20] K. Kanjilal and D. Blume, Phys. Rev. A 73, 060701(R) (2006).
- [21] E. Braaten and H.-W. Hammer, Phys. Rev. A 67, 042706 (2003).
- [22] J. H. Macek, J. Phys. B 1, 831 (1968).
- [23] F. Cabral and L. W. Bruch, J. Chem. Phys. **70**, 4669 (1979).
- [24] D. Blume, Phys. Rev. B **72**, 094510 (2005).